

Motion Artifact Removal by Retrospective Resolution Reduction (MARs)

C. Bookwalter¹, N. Seiberlich¹, M. Griswold^{1,2}, and V. Gulani¹

¹Department of Radiology, University Hospitals Case Medical Center, Cleveland, OH, United States, ²Department of Biomedical Engineering, Case Western Reserve University, Cleveland, OH, United States

Introduction: Motion artifacts in MR images often appear as ghosting or streaking which can obscure clinical information. MR abdominal imaging is especially adversely affected by motion artifacts due to breathing. Even with parallel imaging and fast sequences, breath-holds are often long and difficult for patients. In addition, failed breath-holds are identified only after image acquisition, and no robust method for salvaging the images is available, a critical problem in post-contrast imaging. Assuming that a patient can initially hold their breath but may fail sometime during acquisition, there will be a transition between uncorrupted data and data corrupted by motion. If this transition can be identified, it could be used to eliminate data acquired after motion commenced, providing an avenue for salvaging a useful exam despite poor breath-holds. In this study, the transition between motion free and motion corrupted data is identified by employing a novel algorithm called Motion Artifact Removal by Retrospective Resolution Reduction (MARs) on a centric ordered 3D fat saturated (FS) gradient echo acquisition, where k-space data corrupted by motion are automatically eliminated using processing based on parallel imaging. This method yields an image uncorrupted by motion artifacts, albeit with lower resolution. 3D FS gradient echo imaging was chosen as the first application as this sequence is used for contrast enhanced examinations in the abdomen and is the most critical sequence in a body imaging exam.

Theory: The general proposed MARs algorithm is shown in Figure 1. A single partition of multi-coil, 3D fat-saturated VIBE [1] data set is entirely duplicated using GRAPPA [2] in order to obtain GRAPPA navigators [3-5]. Each collected phase encoding (PE) line in k-space has an equivalent GRAPPA reconstructed PE line. When the acquired PE line and the navigator are compared, the correlation coefficient in presence of motion will be much smaller than without motion. Using this change in correlation coefficient, a transition between corrupted and uncorrupted data is identified. Data collected after the transition are replaced with zeros leading to significant motion artifact removal at the expense of a small decrease in effective resolution. A centric ordered scan will ensure that the center of k-space is acquired during the motion uncorrupted period and the motion corrupted data will be limited to high frequency data at the edges of k-space.

Methods: In this IRB compliant study, fully sampled centric ordered 3D VIBE datasets through the abdomen were obtained for 3 volunteers on a Siemens 1.5T Espree scanner without contrast and for 11 patients on a Siemens Avanto 1.5T scanner post contrast. Multiple data sets were acquired such that each volunteer resumed breathing when approximately 20%, 50%, 70%, and 100% of the data were acquired and similarly patients resumed respiration after 30%, 60%, and 100% of the data were acquired. The center partition of each 3D data set was entirely duplicated with GRAPPA (using 10 ACS lines and a 4x3 GRAPPA kernel size) in order to obtain GRAPPA navigators for each collected PE line. Correlation coefficients were calculated for each pair of PE lines (i.e., acquired and navigator). A boxcar function was fit to the correlation coefficients to identify the transition from motion free data to motion corrupted data. PE lines acquired after the identified transition were replaced with zeros. The images were then reconstructed with the Fourier transform.

Results: Correlation coefficients demonstrate an abrupt decrease at the transition from breath-hold to motion corrupted data. This transition was successfully identified by a least squares fitted boxcar function. Figure 2 shows an example of calculated correlation coefficients (dotted lines) and fitted boxcar function (solid lines) from a patient data set for 30% (blue), 60% (red), and 100% (green) breath-hold. For the example shown, the transitions occur at PE line numbers 52 and 104, or approximately 40% of the full breath-hold. Single partition reconstructions for the same patient are shown in Figure 3, where Figure 3a and 3b are the uncorrected and corrected images, respectively, for the same patient data shown in blue and red in Figure 2. In Figure 3b, note the ascending colon anterior to the liver (arrow) is clearly depicted in the corrected image but poorly visualized in the uncorrected image (Figure 3a). Removal of motion corrupted data resulted in images free of respiratory motion artifacts and with only a slight resolution reduction compared to the intended resolution.

Discussion/Conclusion: MARs was shown to be capable of detecting the transition between breath-hold and free breathing during a centric ordered 3D acquisition, allowing recovery of motion free images with only a small theoretical compromise in resolution. This is a practical clinical solution, since the ideal high resolution image is not of diagnostic value if the patient cannot hold their breath. MARs is instead able to achieve the ideal *practical* resolution for a given patient's breathhold capability. As can be seen in Figure 3, diagnostic information obscured by motion can be recovered using MARs. The method allows the generation of clinically useful images even in the presence of motion, in a robust, fully automated, retrospective manner. It also makes possible an alternative protocol option where the patient provides the longest breath-hold they can over a lengthy acquisition, and the images are reconstructed to include the data collected during the motion free period, yielding the highest resolution exam possible. Initial results with such a protocol (not shown) yield viable images at higher resolution than in our present clinical standard.

References: [1] Rofsky et. al., Radiology, 212(3); 876-884. [2] Griswold et. al., MRM, 47(6); 1202-1210. [3] Bydder et. al., MRM, 49(3); 493-500. [4] Roder et. al., ISMRM 2008, 1291. [5] Lin, et. al., MRM, 2010, 63(2); 339-348.

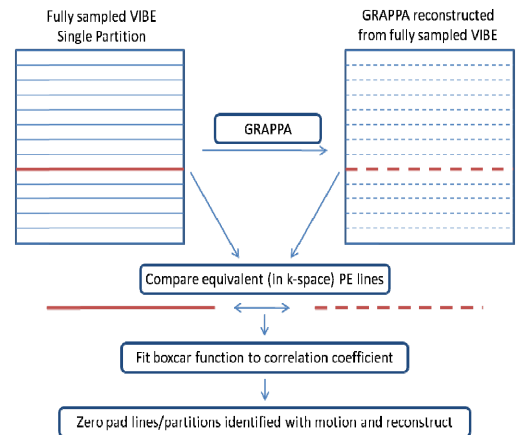


Figure 1: Algorithm flow chart

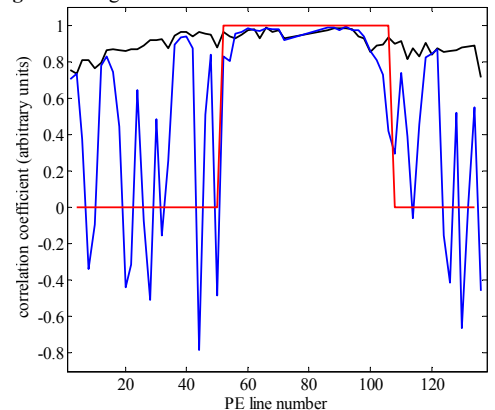


Figure 2: Correlation coefficients (blue) and the fitted boxcar function (red) are shown for a single patient for approximately 30% breath-hold. Full breath-hold correlation coefficients are shown for reference in black.

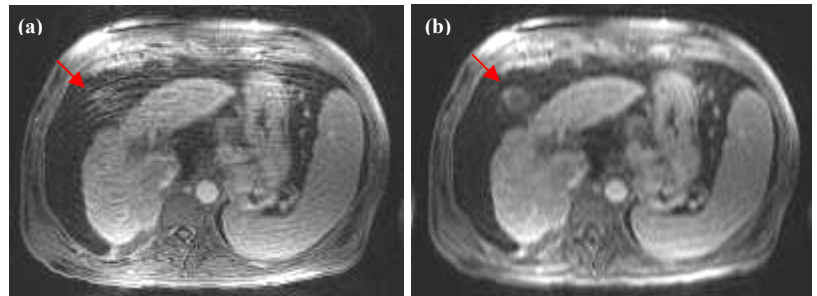


Figure 3: Motion corrupted (a) and motion artifact reduced (b) images in a cirrhotic patient. Note the ascending colon, which is severely distorted by motion artifact in (a) but is clearly visualized in (b).